Analytical Calculation of the 3D Magnetic Field Created by Non-Periodic Permanent Magnet Arrays

He Zhang*, Baoquan Kou, and Liyi Li*****

Abstract – In this paper, the three-dimensional magnetic field created by non-periodic magnet arrays is calculated analytically. The analytical expression of the magnetic field is derived by using a magnetic charge model. The influence of ferromagnetic boundaries is formulated with an image method. Finally, we compare the results determined by analytical calculations to those from a finite element simulation.

Keywords: Analytical calculation, Magnetic field, Permanent magnet arrays

1. Introduction

Permanent magnet arrays are widely used in some operating actuators such as linear motors and planar motors. These devices often consist of a periodic permanent magnet array as shown in Fig. 1 (a) (b) in order to obtain a large traveling range. A common method to analyze this type of permanent magnetic array is to solve the Laplace equation under the assumption that the magnetic array is infinite [1]. However, this method is not accurate enough for some short-stroke precision actuators with non-periodic arrays as shown in Fig. 1 (c) (d) due to disregard of the real fringe field. In this paper, an analytical method based on the concept of magnetic charge and the method of image [2-7] is employed for calculating the magnetic field of non-periodic arrays.

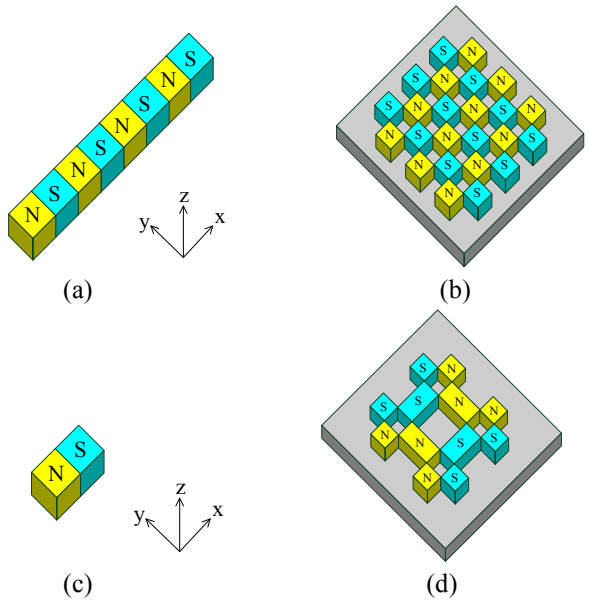

Fig. 1. Permanent magnet arrays. (a) periodic linear. (b) periodic planar. (c) non-periodic linear. (d) non-periodic planar

2. Analytical Model

2.1 Magnetic Field Due to a Parallel Magnetized PM

According to equivalent magnetic charge method, the effect of magnetization for a parallel uniform magnetized magnet can be represented by two magnetic charge surfaces on the sides of the permanent magnet, which are perpendicular to the magnetization direction. Fig. 2 shows the equivalent magnetic charge model of the magnet which is magnetized in the z direction. The expression of the magnetic charge surface density σ_m is

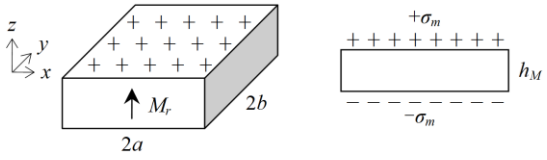

Fig. 2. The equivalent magnetic charge model

$$\sigma_m = \mu_0 \vec{M}_r \cdot \vec{n} \tag{1}$$

where M_r is the magnetization of the permanent magnet.

Differential magnetic charge is expressed as

$$dQ_m = \sigma_m ds \tag{2}$$

* Department of Electrical Engineering, Harbin Institute of Technology,China. (antonyamanda@163.com)

Received 29 February 2012; Accepted 07 August 2012

where *ds* is the cross section of magnetization direction.

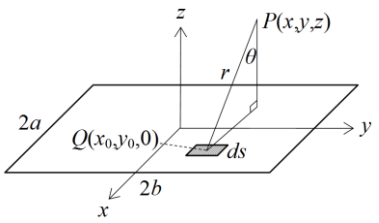

Fig. 3. Geometrical illustration of the magnetic field calculation

Differential magnetic field intensity is

$$d\vec{H} = \frac{\sim^{m}}{4\pi\mu_0 r^2}\vec{a}_r \tag{3}$$

where r is the distance between the origin and an arbitrary observation point.

As shown in Fig. 3, the z axis component of magnetic field intensity is

$$dH_z = d\vec{H}\cdot\cos\theta \tag{4}$$

where

$$\cos\theta = \frac{z}{r} = \frac{z}{\sqrt{(x-x_0)^2+(y-y_0)^2+z^2}} \tag{5}$$

The magnetic field intensity in the point P(x, y, z) created by the positive charge surface $2a\times 2b$ can be obtained as

$$H_z = \int_{-b}^{b}\int_{-a}^{a}\frac{M_r}{4\pi}\cdot\frac{z}{[(x-x_0)^2+(y-y_0)^2+z^2]^{3/2}}dx_0\cdot dy_0 \tag{6}$$

Through mathematical derivation, Eq. (6) can be expressed as

$$\begin{aligned} H_z = &-\frac{M_r}{4\pi}\cdot\text{arctg}\frac{(a-x)(y-y_0)}{z\sqrt{[(a-x)^2+(y-y_0)^2+z^2]}}\Big|_{y_0=-b}^{y_0=b} \\ &-\frac{M_r}{4\pi}\cdot\text{arctg}\frac{(a+x)(y-y_0)}{z\sqrt{[(a+x)^2+(y-y_0)^2+z^2]}}\Big|_{y_0=-b}^{y_0=b} \end{aligned} \tag{7}$$

By adding the negative charge surface, the analytical expression of the three dimensional magnetic field created by a parallel magnetized PM can be obtained as

$$B_z = K\times\begin{bmatrix} \zeta(a-x,b-y,z-h_M)+ \\ \zeta(a-x,b+y,z-h_M)+ \\ \zeta(a+x,b-y,z-h_M)+ \\ \zeta(a+x,b+y,z-h_M)- \\ \zeta(a-x,b-y,z)-\zeta(a-x,b+y,z)- \\ \zeta(a+x,b-y,z)-\zeta(a+x,b+y,z) \end{bmatrix} \tag{8}$$

Where

$$K = \frac{\mu_0 M_r}{4\pi} \tag{9}$$

$$\zeta(\zeta_1,\zeta_2,\zeta_3) = \text{arctg}\frac{\zeta_1\cdot\zeta_2}{\zeta_3\cdot\sqrt{\zeta_1^{\,2}+\zeta_2^{\,2}+\zeta_3^{\,2}}} \tag{10}$$

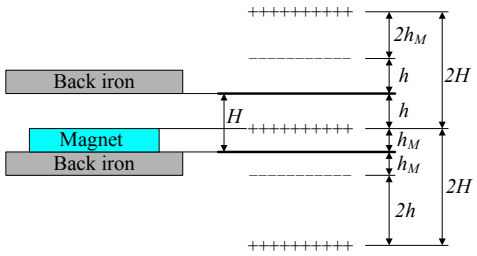

(a)

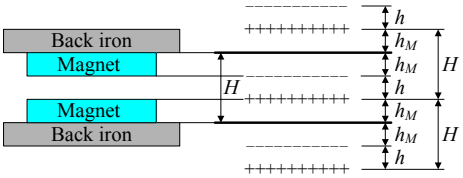

(b)

Fig. 4. Concept of image method. (a) Single side and (b) Double sides

2.2 Method of Images

In a linear or planar motor, each magnetic pole is sandwiched between the surfaces formed by the iron cores. The final air-gap field distribution is determined by both permanent magnets and ferromagnetic boundaries. If each elemental magnetization at the magnet surface is regarded as a magnetic charge, the flux density in the air space can be computed by applying the method of images. Fig. 4 shows the concept of the image method. The effect of boundaries on fields may be replaced by a series of images. The major assumptions used in deriving the analytical model are as follows:

1) The area and thickness of the ferromagnetic boundaries are infinite;

2) Permeability of the back iron is infinite;

3) The magnetization curve of the permanent magnet is

linear;

4) Relative recoil permeability of the permanent magnet μr is equal to 1.

Making use of coordinate transformation and the superposition principle, we can derive the image field. The real magnetic field is the sum of the contributions of each image charge and the original charge. The analytical expression of magnetic field created by a magnet under two parallel ferromagnetic boundaries in Fig.4 a) is derived as

$$B_z = K \times \begin{bmatrix} \zeta(a-x,b-y,z-h_M)+ \\ \zeta(a-x,b+y,z-h_M)+ \\ \zeta(a+x,b-y,z-h_M)+ \\ \zeta(a+x,b+y,z-h_M)- \\ \zeta(a-x,b-y,z+h_M)- \\ \zeta(a-x,b+y,z+h_M)- \\ \zeta(a+x,b-y,z+h_M)- \\ \zeta(a+x,b+y,z+h_M) \end{bmatrix} + K \times \sum_{i=1}^{\infty} \begin{bmatrix} \zeta(a-x,b-y,z-h_M \pm i \cdot 2H)+ \\ \zeta(a-x,b+y,z-h_M \pm i \cdot 2H)+ \\ \zeta(a+x,b-y,z-h_M \pm i \cdot 2H)+ \\ \zeta(a+x,b+y,z-h_M \pm i \cdot 2H)- \\ \zeta(a-x,b-y,z+h_M \pm i \cdot 2H)- \\ \zeta(a-x,b+y,z+h_M \pm i \cdot 2H)- \\ \zeta(a+x,b-y,z+h_M \pm i \cdot 2H)- \\ \zeta(a+x,b+y,z+h_M \pm i \cdot 2H) \end{bmatrix} \quad (11)$$

The field created by a couple of magnets in Fig.4 b) is derived as

$$B_z = K \times \begin{bmatrix} \zeta(a-x,b-y,z+h/2)+ \\ \zeta(a-x,b+y,z+h/2)+ \\ \zeta(a+x,b-y,z+h/2)+ \\ \zeta(a+x,b+y,z+h/2)- \\ \zeta(a-x,b-y,z-h/2)- \\ \zeta(a-x,b+y,z-h/2)- \\ \zeta(a+x,b-y,z-h/2)- \\ \zeta(a+x,b+y,z-h/2) \end{bmatrix} + K \times \sum_{i=1}^{\infty} \begin{bmatrix} \zeta(a-x,b-y,z+h/2 \pm i \cdot H)+ \\ \zeta(a-x,b+y,z+h/2 \pm i \cdot H)+ \\ \zeta(a+x,b-y,z+h/2 \pm i \cdot H)+ \\ \zeta(a+x,b+y,z+h/2 \pm i \cdot H)- \\ \zeta(a-x,b-y,z-h/2 \pm i \cdot H)- \\ \zeta(a-x,b+y,z-h/2 \pm i \cdot H)- \\ \zeta(a+x,b-y,z-h/2 \pm i \cdot H)- \\ \zeta(a+x,b+y,z-h/2 \pm i \cdot H) \end{bmatrix} \quad (12)$$

3. Model Verification

In order to verify the accuracy of the analytical expression, a comparison between the analytical calculation and simulation is carried out. The simulation results of the magnetic field are obtained by the FEM software--Ansoft3D.

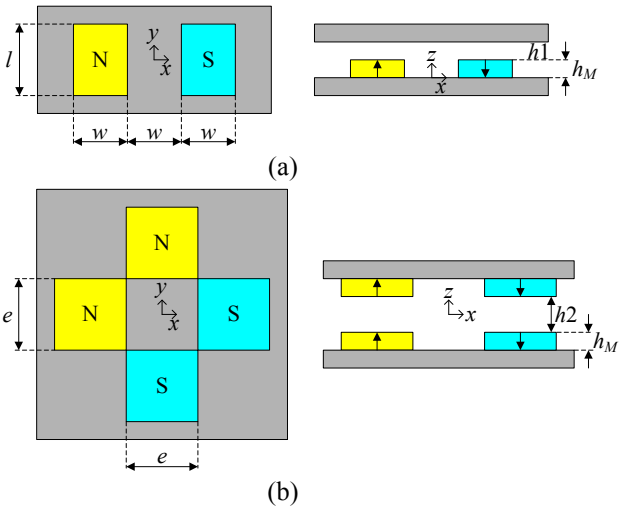

Fig. 5. Magnet array examples. (a) One-dimension single-sided array and (b) Two-dimension double-sided array

Table 1. Dimensions and material properties of magnet arrays

Symbol	Value	Unit
l	20	mm
w	15	mm
e	20	mm
h_M	5	mm
$h1$	5	mm
$h2$	10	mm
B_r	1.118	T

Table 2. Coordinate values of auxiliary lines

	lines	x	y	z	Unit
array 1	1	[-40,40]	0	6	mm
	2	[-40,40]	0	7.5	mm
	3	[-40,40]	5	7.5	mm
	4	[-40,40]	10	7.5	mm
array 2	1	[-40,40]	0	0	mm
	2	[-40,40]	0	1	mm
	3	[-40,40]	0	2.5	mm
	4	[-40,40]	0	4	mm
	5	[-40,40]	5	2.5	mm
	6	[-40,40]	10	2.5	mm

3.1 Two Magnet Array Examples

Two non-periodic magnet array examples are adopted to verify the field equations discussed above. The first single-sided array consists of 2 alternating-pole magnets. The second double-sided array, which is a two-dimensional array, consists of 4 square magnets. The uniform magnetization is along the z direction, and l, w, e and hM are the dimensions of the magnets. The magnet arrangement and parameters are shown in Fig. 5. The coordinate system of magnet array 1 is located at the centric of the back iron surface. The coordinate system of magnet array 2 is located in the center of the air-gap. Table I lists the geometric values and magnetic properties.

3.2 Comparison with FE Analysis

Fig. 6 and Fig. 7 show the 3D magnetic field distribution of the two magnet arrays respectively. The calculated magnetic flux densities are obtained by employing Eq. (11) and Eq. (12).

In order to better illustrate the agreement between calculating and simulating values, several auxiliary lines are set for field comparison. This is shown in table II. Fig. 8 and Fig. 9 show the comparison curves of magnetic field for the auxiliary lines. By contrast, it can be concluded that the magnetic field analysis using the magnetic charge method and the image method is in good agreement with FEM.

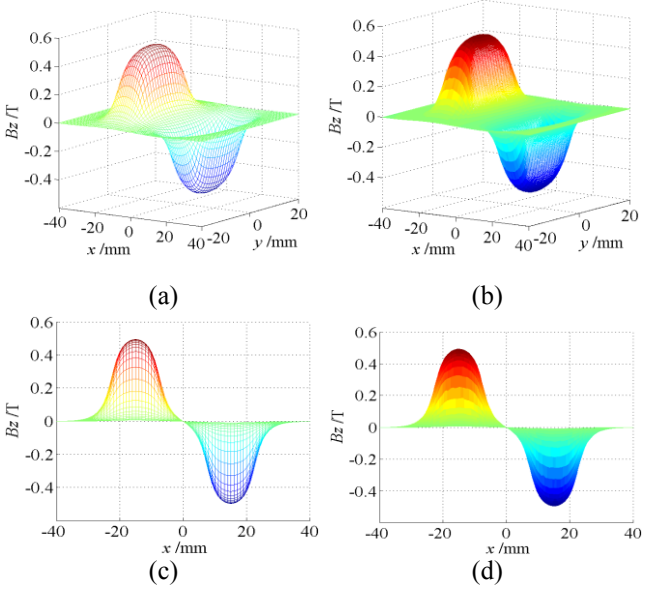

Fig. 6. 3D magnetic field distribution of magnet array 1. (a) calculation result. (b) FE simulation result. (c) side view of calculation result. (d) side view of FE simulation result.

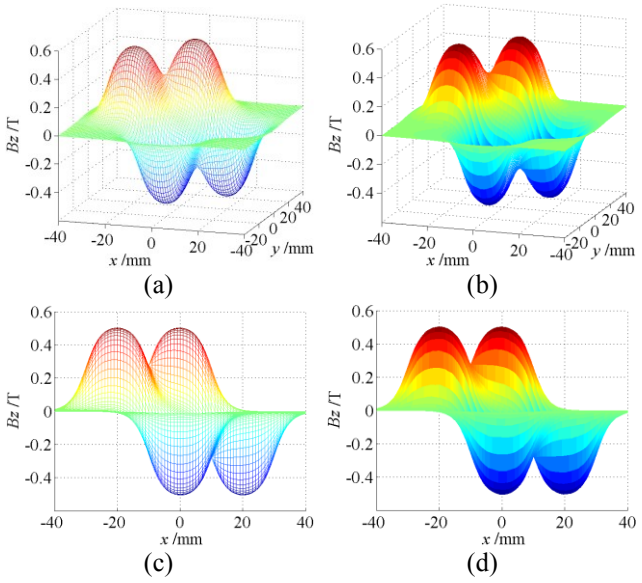

Fig. 7. 3D magnetic field distribution of magnet array 2. (a) calculation result. (b) FE simulation result. (c) side view of calculation result. (d) side view of FE simulation result.

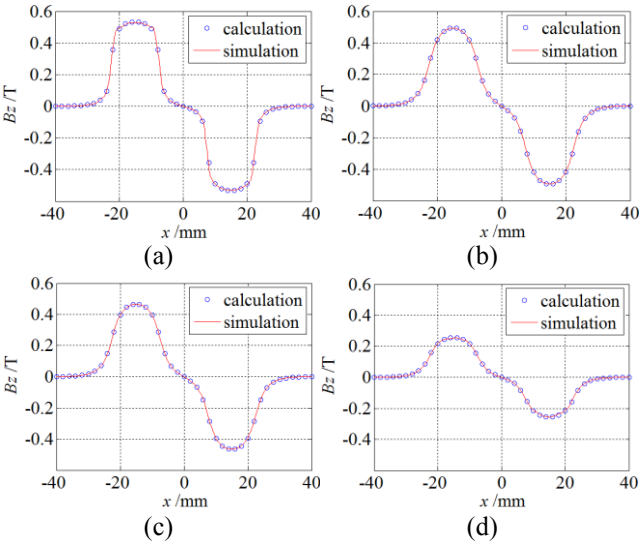

Fig. 8. Comparison of analytical calculation and FE simulation of the magnetic field created by magnet array 1. (a) y=0mm, z=6mm. (b) y=0mm, z=7.5mm. (c) y=5mm, z=7.5mm. (d) y=10mm, z =7.5mm.

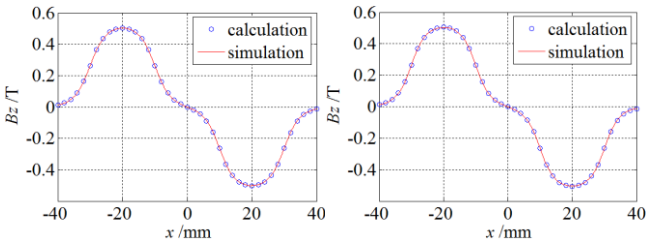

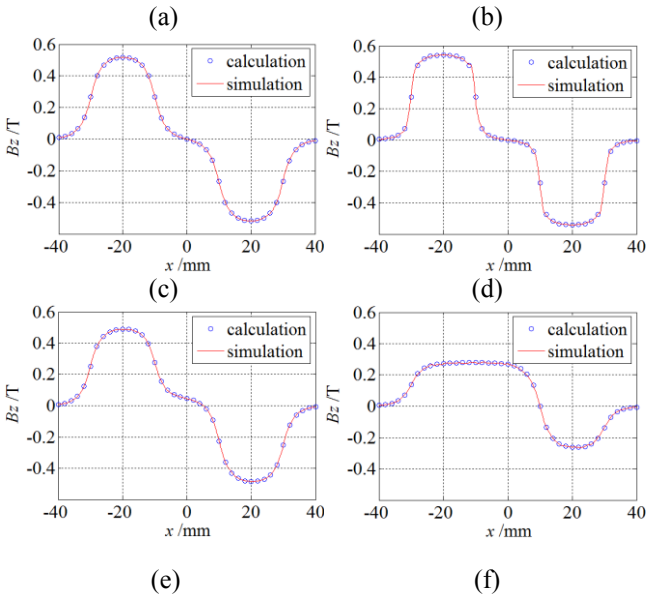

Fig. 9. Comparison of analytical calculation and FE simulation of the magnetic field created by magnet array 2. (a) y=0mm, z=0mm. (b) y=0mm, z=1mm. (c) y=0mm, z=2.5mm. (d) y=0mm, z=4mm. (e) y=5mm, z=2.5mm. (f) y=10mm, z=2.5mm.

4. Conclusion

In this paper, an analytical method for computing the 3D magnetic field of non-periodic permanent magnet arrays has been presented. By using the method of images and the concept of magnetic charges, the air-gap field can be obtained to a good degree of accuracy. Agreement between calculation and simulation results is satisfactory, thus verifying the validity of the proposed analytical method. The analytical method is also computationally efficient and time saving compared with 3D finite element methods.

Acknowledgements

The work described in this paper was supported by the National S&T Major Project (2009ZX02207-001) and Program for New Century Excellent Talents in University (NCET-08-0158).

References

[1] H. S. Cho, C. H. Im, and H. K Jung, "Magnetic field analysis of 2-D permanent magnet array for planar motor," IEEE Transactions on Magnetics, Vol. 37, No. 5, pp. 3762–3766, September 2001.

[2] S. A. Nasar and G. Y. Xiong, "Determination of the field of a permanent magnet disk machine using the concept of magnetic charge," IEEE Transactions on Magnetics, Vol. 24, No. 3, pp. 2038-2044, May 1988.

[3] S. H. Lee, S. B. Park, S. O. Kwon, J. Y. Lee, J. J Lee, J. P Hong, and J Hur, "Characteristic analysis of the slotless axial-flux type brushless dc motors using image method," IEEE Transactions on Magnetics, Vol. 42, No. 4, pp. 1327–1330, April 2006.

[4] H. Allag, J-P. Yonnet, M. E. H. Latreche. "3D analytical calculation of forces between linear halbach-type permanent magnet arrays," 8TH International Symposium on Advanced Electromechanical Motion Systems, pp. 382-387, 2009.

[5] R. Engel-Herbert, T. Hesjedal, "Calculation of the magnetic stray field of a uniaxial magnetic domain," Journal of Applied Physics, Vol. 97, No. 7, pp. 1-4, 2005.

[6] T-F. Chan, L. L. Lai, "Computation of air-gap field in an axial-flux permanent-magnet machine using the method of images," IEEE International Electric Machines and Drives Conference, pp. 1647-51, 2009.

[7] D. Golda, M. L. Culpepper, "Modeling 3D magnetic fields for precision magnetic actuators that use non-periodic magnet arrays," Precision Engineering, Vol. 32, No. 2, pp. 134–142, 2008.

He Zhang received B.E. and M.E. degrees from Harbin Institute of Technology, Harbin, China, in 2008 and 2010, respectively. His research interests are planar motors of high positioning accuracy and high response.

Baoquan Kou received B.E. and D.E. degrees from Harbin Institute of Technology, Harbin, China, in 1992 and 2004, respectively, and the M.E. degree from Chiba Institute of Technology, Chiba, Japan, in 1995. From 2007, He is a professor in the School of Electrical Engineering and Automation, HIT. His research areas are electric drives of electric vehicles, linear motors and linear electromagnetic drives, control of power quality, and superconducting motors.

Liyi Li received B.E., M.E., and D.E. degrees from Harbin Institute of Technology, Harbin, China, in 1991, 1995, and 2001, respectively. From 1991 to 1993, he worked in the Science and Technology Development General Company of HIT. From 2002 to 2004, he worked in the mobile station for the post-doctors of Dalian University of Technology, Dalian, China. From 2004, he has been a professor in the School of Electrical Engineering and Automation, HIT. His research areas are control and drive of linear electromagnetic systems, linear electromagnetic launches, accumulation of electric energy, and superconducting motors.